Iron dynamics in Al–Cu–Fe quasicrystals and approximants: Mössbauer and neutron experiments

2009 J. Phys.: Condens. Matter 21 045405

(http://iopscience.iop.org/0953-8984/21/4/045405)

J. Phys.: Condens. Matter **21** (2009) 045405 (15pp) doi:10.1088/0953-8984/21/4/045405

Iron dynamics in Al–Cu–Fe quasicrystals and approximants: Mössbauer and neutron experiments

R A Brand[1,2], **F Hippert**[3] **and B Frick**[4]

[1] INT, Forschungszentrum Karlsruhe, D-76344 Eggenstein-Leopoldshafen, Germany
[2] Department of Physics, Universität Dusburg-Essen, D-47048 Duisburg, Germany
[3] Laboratoire des Matériaux et du Génie Physique, CNRS, Institut Polytechnique de Grenoble, BP 257, F-38016 Grenoble Cédex 1, France
[4] Institute Laue-Langevin, BP 156, F-38042 Grenoble Cédex 9, France

E-mail: richard.brand@uni-due.de

Received 5 September 2008, in final form 7 December 2008
Published 8 January 2009
Online at stacks.iop.org/JPhysCM/21/045405

Abstract

We present new results on the iron dynamics in the icosahedral quasicrystal i-AlCuFe and two cubic approximants as well as the non-approximant Al–Cu–Fe cubic B2 phase. Conventional Mössbauer spectroscopy is used as well as, for the i-AlCuFe phase, high Doppler velocity Mössbauer spectroscopy and quasielastic neutron scattering for samples with different Fe isotope contents. We show that in the i-phase the Fe Lamb–Mössbauer recoilless fraction decreases below that predicted for lattice vibrations alone for temperatures above about 550 K. This decrease is correlated with the onset of a quasielastic signal seen in both Mössbauer and neutron backscattering spectroscopy, which indicates the presence above 550 K of Fe jump processes confined in a local cage. The timescale of the Fe jumps (660 ps at 1000 K) and their temperature dependence differ widely from those of Cu jumps in the same i-AlCuFe quasicrystal. From the temperature dependence of the quadrupole splitting of the ^{57}Fe Mössbauer spectrum, one can distinguish two kinds of Fe jumps, one starting at 550 K and the second above 800 K. In the two cubic approximants, a loss in the Fe recoilless fraction also occurs above 550 K, revealing the same kind of Fe dynamics as in the i-phase but the effect is smaller. On the other hand, no anomalous Fe dynamics (other than lattice vibrations) is detected in the B2-AlCuFe phase. Since the cubic approximants possess similar local configurations as the quasicrystal, we conclude that locally a Penrose tile description is appropriate. This shows that the detected Fe jumps can be interpreted in terms of phason-like local tiling flips.

(Some figures in this article are in colour only in the electronic version)

1. Introduction

After the discovery of quasicrystals (QCs), which have non-periodic long range order and non-crystallographic icosahedral point symmetry [1], it was obvious that this new type of order might lead to original lattice dynamical properties in addition to conventional phonons. Indeed, new low energy topological defects, termed phasons, have been predicted [2–6]. Reviews of the present understanding of phasons can be found in [7] as well as the proceedings of the Jubilee Conference [8].

Phasons are also involved in deformation behaviour of QCs. Information on phasons is required to clarify questions on phase stability and diffusion [9], as well as QC ↔ periodic approximant phase changes.

Aperiodic phases (consisting of incommensurably modulated phases, composites and quasicrystals) display sharp diffraction peaks having a Fourier module with dimensionality higher than physical space. Such structures can be described as periodic in a higher dimensionality with atomic positions given by the intersection of this higher-dimensional space with the real physical space, denoted as parallel space. The additional spatial dimensions are denoted as perpendicular space. Atoms become surfaces in this description, extended in perpendicular space. As a result of this higher-dimensional periodicity,

new modes appear related to the phase of this intersection (cut). These excitations are termed phasons. In quasiperiodic structures, the atomic surfaces are in addition discontinuous, so that phasons involve stoichiometry-preserving atomic jumps from one atomic surface to a neighbouring one.

Phason elasticity in the ('coarse grained') hydrodynamic limit has received intense theoretical treatment [10, 11]. In a generalized linear elastic theory, the displacements v_i become u_i in parallel and w_i in perpendicular space, $v_i = (u_i, w_i)$. The phonon, phason and phonon–phason coupling terms of the elastic free energy have been studied for a number of different models. (For the following discussion see [12].) Due to the discontinuous atomic surfaces the strain ∇w_i (phason strain) results in non-infinitesimal atomic jumps between neighbouring atomic surfaces of some atoms or groups of atoms. These are termed phason jumps. Even for coherent long wavelength phason modes, these atoms or groups will be relatively separated from each other. The hydrodynamic theory [10] results in a dynamical phason relaxation. From the equipartition theorem, the mean square fluctuations in **v** are given by

$$\langle v_i(q) v_j(q) \rangle = k_B T K_{ij}^{-1}, \tag{1}$$

where K_{ij} is the kinetic matrix describing the dynamics. This leads to thermal fluctuations in phason fields with an associated Debye–Waller factor. Such effects have been observed in x-ray diffraction [13, 14]. Since the Fourier transform $K_w(q) \sim q^2$, large q modes with short wavelength should decay quickly while small q modes with long wavelength should decay slowly. Slow decay has been seen by Francoual *et al* using x-ray photo-correlation spectroscopy [15, 16]. They find a q^2 dependence of the decay, as well as decay times of the order of several tens of seconds. Dislocation motion in quasicrystals is regulated by phason motion. Feuerbacher and Caillard [17] have reported relaxation results using transmission electron microscopy. They find decay times of fringe patterns due to moving dislocations of the order of 1000 s. Extensive studies have also been presented of diffuse scattering of neutrons and synchrotron radiation (for example, see [18–21]), with similar results for a q^2 dependence. This has also been interpreted as being due to long wavelength phason dynamics. However, it has also recently been shown that these properties (q^2 dependence of satellite peaks, slow relaxation) can also be obtained in a model not invoking coherent long range phasons, but just local atomic displacements following the icosahedral symmetry [22].

In the present work we focus on local atomic jumps. For short wavelength fast phason modes as well as phason-like local atomic dynamics, a more local model respecting icosahedral symmetry rather than coherent phason modes is helpful. This is the case of the Penrose tiling where a phason can be described as a local tile rearrangement. Here we will denote such rearrangements as tiling flips. (In the literature differing phason nomenclature has led to some confusion: see [12, 23] for discussions.)

Atomic jumps can be detected through a measurement of the dynamical structure factor $S(\vec{Q}, \omega)$ with $\vec{Q}$ the scattering wavevector and $\hbar\omega$ the energy transfer. They lead to a quasielastic (QE) scattering centred at zero energy transfer [24–26], the characteristics of which give information on the jump timescale and range. Of course all atomic jumps are not related to tiling flips. Indeed a description of local degrees of freedom in terms of phasons is relevant when a quasiperiodic or perpendicular space description is necessary [12]. A clear counterexample can be found in the work of Vogl and co-workers [27–29] who observed fast atomic jumps in some crystalline systems in which one atom is connected to a cage of nearby possible sites. This kind of motion is sometimes denoted cage diffusion in the literature. It should not be confused with the long ranged diffusion processes which also involve atomic jumps. Note that the characteristics of the QE signal allow us in principle to distinguish between cage and long ranged diffusion. Examples have been given, for instance, in [27–29].

There have been extensive studies of dynamical properties in i-AlCuFe and i-AlPdMn QCs by QE neutron scattering [30–33]. The dependence of the dynamical structure factor on the $\vec{Q}$ direction could be studied in single crystals of i-AlPdMn QC [33]. In the isostructural system i-AlCuFe, only $S(Q, \omega)$ (with $Q = |\vec{Q}|$) could be investigated due to the lack of large enough single crystals. However, in i-AlCuFe it is possible to use isotopic substitution (Cu and Fe) [30, 32] as well as the Mössbauer effect on Fe [34–36]. This yields atomic-specific information on the dynamics. A summary of previous studies in i-AlCuFe is given below.

One Cu jump was first observed for temperatures $T \geqslant 723$ K in time-of-flight neutron scattering experiments [30] through the detection of a QE line with a temperature-independent full width at half-maximum (FWHM) $\Gamma_{QE} = 110\ \mu$eV. This corresponds to a timescale $\tau = 12$ ps. Following [32] and ignoring model-dependent numerical factors, τ is estimated here as $2\hbar/\Gamma_{QE}$. (Note that [30–33] as well as [36] report the half-width at half-maximum for all detected QE lines.) This timescale must be understood as an average residence time between jumps. The length scale of this Cu jump, from the Q dependence, is 4 Å. Another Cu jump with $\Gamma_{QE} = 500\ \mu$eV, and hence $\tau = 2.6$ ps, and a length scale smaller than 1.9 Å was detected above 900 K [32]. The temperature dependence of these two Cu jumps was found to be very unusual, with an almost constant timescale but a temperature-dependent Arrhenius-like amplitude. This is contrary to the usual result where the timescale changes strongly with temperature. Thus it seems from this result that the detected copper jumps are very fast and at least not strongly temperature-dependent, but that the possibility of jumping is regulated by a second process (for example, a neighbouring atom) [32]. A much wider QE contribution ($\Gamma_{QE} \sim 1800\ \mu$eV) ascribed to all atomic species was also found at 1043 K [32]. Finally the existence of another jump was detected at 1043 K in neutron backscattering experiments [32]. Its energy scale is of 4 μeV, i.e. its timescale (330 ps) is much longer than the previous ones. Using isotopic substitution, it was observed that the QE intensity did not change with the scattering cross section of copper, so that Cu is not involved in this latter process. However, its atomic nature (Al, Fe or both) remained uncertain. Using high velocity ^{57}Fe Mössbauer spectroscopy, Coddens *et al* [36] were able to detect a broad QE line

on an energy scale of about 4 μeV at 1060 K. This is an unambiguous signature of iron jumps. However, neither their temperature dependence nor their possible relationship with the low energy jump detected in neutron backscattering experiments were studied. This vast difference in timescales, of about two orders of magnitude, in the copper and iron jumps in the same QC structure has remained a puzzle. In this study we present both low and high velocity Mössbauer spectroscopy (MS) as well as neutron scattering (NS) results on the i-AlCuFe phase. Our goal is to investigate the iron dynamics in this QC.

Another objective of the present work was to compare the dynamics in QCs and in periodic phases, both simple phases and approximants, in order to clarify the role of local environments and quasiperiodicity. This is an important point, which has received only little attention in the literature so far. Approximants are crystalline phases with unusually large unit cells. Their structural properties, such as local order, approach those of the QC when p/q, which designates the order of the approximant, approaches the golden mean. Long wavelength coherent phason modes are not expected in approximants since strict quasiperiodic order is necessary for such modes. This has been demonstrated by a study of the ZnMgSc QC and its ZnMg 1/1 approximant [37] by x-ray diffuse scattering. Phason modes could only be observed in the QC but not in the 1/1 approximant, consistent with the hydrodynamical theory. However, local processes are not at all ruled out by this requirement and in fact can be expected to exist in approximants given their similar local nature. The AlCuFe system is especially well suited for such a study. Both approximants and simple crystalline phases with compositions close to those of the QC phase [38–40] exist. Hence we could compare by MS the Fe dynamics in the i-AlCuFe QC to that in two cubic 1/1 approximants (denoted α and α') as well as in a conventional cubic B2 phase.

In conventional (low Doppler velocity) Mössbauer spectroscopy, indirect information on atomic jumps can be gained from the temperature dependence of the central elastic line, giving the Lamb–Mössbauer (L–M) recoilless fraction $f(T)$. As discussed in the appendix, phonons lead to a linear decrease in $\ln f(T)$ at high temperatures which in the Debye model depends on the Debye temperature. Additional modes of atomic motion lead to a further decrease in $\ln f(T)$ as soon as their energy range exceeds that of the elastic line. High temperature Mössbauer studies of i-AlCuFe have been presented by Janot *et al* [34] and de Araújo *et al* [35]. In both cases, an anomalous decrease in $\ln f(T)$ is reported at high temperature but not compared to models. Here we analyse the temperature dependence of $\ln f(T)$ by comparing it with the expected behaviour for phonons and by correlating it to the temperature dependence of the QE line detected in high Doppler velocity MS. A study of the temperature dependence of the quadrupole splitting of the ^{57}Fe Mössbauer resonance, measuring the electric field gradient (EFG), is presented as well. The effective EFG in the dynamical limit is sensitive to changes in orientation of the principal EFG tensor axes occurring, for example, for certain jumps lacking mirror symmetry. It can then be used to detect properties of such jumps.

2. Samples and experiments

2.1. Samples

All the samples were prepared by planar flow casting methods, as described for instance in [38]. After annealing they were all shown to be single phase by x-ray diffraction. Below is a list of the samples used in this study.

(i) Quasicrystalline i-$Al_{62}Cu_{25.5}Fe_{12.5}$ (annealed 2 h at 1070 K) denoted i-AlCuFe. For this composition, the i-phase is known to be stable up to 1100 K. Two different samples were studied, one containing natural Fe and the other containing 100% ^{57}Fe. These samples were the same ones used in the inelastic x-ray and neutron experiments reported in [41, 42].

(ii) Cubic 1/1 approximants. Substitution of a few per cent of Si for Al leads to the formation of two different low order cubic 1/1 approximants, in distinct composition regions [40]. The first one, denoted α, exists for Cu and Fe concentrations similar to those in QCs and higher-order approximants. The second one, denoted α', is found in a very different concentration domain, for a fixed Fe content (17.5 at.%) and a small amount of Cu (around 4 at.%). The samples studied are α-$Al_{55}Si_7Cu_{25.5}Fe_{12.5}$ (annealed 24 h at 920 K) denoted α-AlSiCuFe and α'-$Al_{76.7}Si_7Cu_{3.8}Fe_{17.5}$ (annealed 72 h at 870 K) denoted α'-AlSiCuFe. These samples were the same ones used in the EXAFS experiments reported in [43]. They both have a large cubic cell parameter, close to 12.4 Å, and about 138 atoms per unit cell.

(iii) Cubic non-approximant B2-type phase (cubic CsCl structure) β-$Al_{52}Cu_{35}Fe_{13}$ (annealed 18 h at 1170 K) denoted β-AlCuFe [44]. Its cubic cell parameter is equal to 2.9 Å. For this composition, Al occupies one crystallographic site and Cu and Fe are randomly distributed on the other.

2.2. Mössbauer experiments

High temperature Mössbauer experiments have been made on *all* samples given in the above list in a Doppler velocity range of about ± 2 mm s^{-1} corresponding to ± 0.096 μeV (14.4 keV gamma ray). The spectrometer resolution is equal to ~ 0.24 mm s^{-1} (FWHM) which is the sum of Γ_0, the natural (FWHM) width of the ^{57}Fe nuclear transition, and of instrumental effects including defects in the drive, etc. Γ_0 is the sum of the source and absorber FWHM ideal widths, each equal to 0.097 mm s^{-1} corresponding to an energy uncertainty of $\Delta_E = 4.6$ neV. A simple oven fitted with Mylar windows was used with a dynamic vacuum of about 10^{-6} Torr. The maximum temperature used was 1070 K for i-AlCuFe, 975 K for β-AlCuFe and only 850 K for the 1/1 approximant phases, which are not as stable as the i-AlCuFe.

In order to search for quasielastic effects, Mössbauer experiments were performed on the ^{57}Fe-enriched i-AlCuFe phase, in the temperature range (300, 1070 K), over a much wider range of Doppler velocities ± 100 mm s^{-1} (corresponding to ± 4.8 μeV). The use of an enriched sample

is necessary to improve the contrast between the non-resonant flat background and any broad quasielastic signal centred on zero energy shift.

For making the Mössbauer absorbers, the ribbons were ground into a powder and mixed with a small amount of high purity BN powder or pressed into BN wafers to better distribute the grains in the oven sample holder. This consists of two BeO wafers pressed together in a tantalum clamp. For each natural Fe sample, the absorber contained about 5 mg cm^{-2} of alloy powder. Thus the Mössbauer absorption thickness parameter [45] t_{ab} was less than one for the natural Fe sample. In order to detect a quasielastic signal in high velocity Mössbauer experiments, much larger values of t_{ab} are required although values larger than unity lead to nonlinear absorption [45], deforming the spectrum lineshape in the central (high absorption) region. The absorbers were made with about 20 mg cm^{-2} alloy powder, so that t_{ab} was about 50.

Although the i-phase is stable up to 1100 K, the precipitation of a small amount of the β-phase is possible above 1020 K when the sample holder is not made of alumina, which is the case here. In addition, slow oxidation of the sample would remove Al from the QC matrix, and also cause some precipitation of the β-phase. In all experiments on i-AlCuFe phases, the samples were checked before and after with room temperature Mössbauer spectra and x-ray diffraction. No detectable amount of β-phase was found. Hence one can firmly assert that no structural evolution of the i-phase occurred in these experiments and that the anomalous temperature dependences reported in the next section are intrinsic properties of the i-phase.

2.3. Neutron scattering experiments

Experiments were performed at 600 and 1050 K on the natural Fe and ^{57}Fe-enriched i-AlCuFe samples on the high-resolution backscattering instrument IN16 [46] at the Institute Laue-Langevin (Grenoble, France). This instrument has an energy resolution (FWHM) of 0.9 μeV at an incident neutron energy of 2.08 meV. The accessible energy range is $\pm$15 μeV and the scattering wavevector Q ranges from 0.02 to 1.9 Å^{-1}. Typical counting times, for one sample at a given temperature, were one day. It was necessary to mask off part of the analyser surface where strong (elastic) Bragg reflection occurred. For these studies, the samples were mounted in hollow cylindrical sample holders made of thin Ta sheets welded to stainless steel flanges. An oven with a dynamic vacuum of about 10^{-7} Torr was used.

3. Results

3.1. Low velocity Mössbauer results

3.1.1. Data analysis. Typical Mössbauer spectra from the samples studied here are shown in figure 1. These are from natural Fe i-AlCuFe but certain general remarks are in order for all the samples. For each spectrum, the area below the flat background level is a measure of the L–M recoilless fraction $f(T)$. The centroid of the spectrum defines the average centre shift. The Mössbauer spectra in figure 1 is a broadened doublet. The line separation results from the partial lifting of the degeneracy of the nuclear excited state $I = 3/2$ due to the interaction between the nuclear quadrupole moment and the electric field gradient (EFG) [45]. The broadening of each line above the spectrometer resolution is due to the overlapping of the contributions of many different local atomic and chemical environments with differing centre shift δ and quadrupole splitting Δ. Analysis of the room temperature spectra shows that the two lines have equal area, as expected from a random powder sample. The observed slight asymmetry of the spectral widths can be explained by a correlation in the variation in the centre shift δ and quadrupole splitting Δ, as we discussed before [47], and seen by others as well [48, 49].

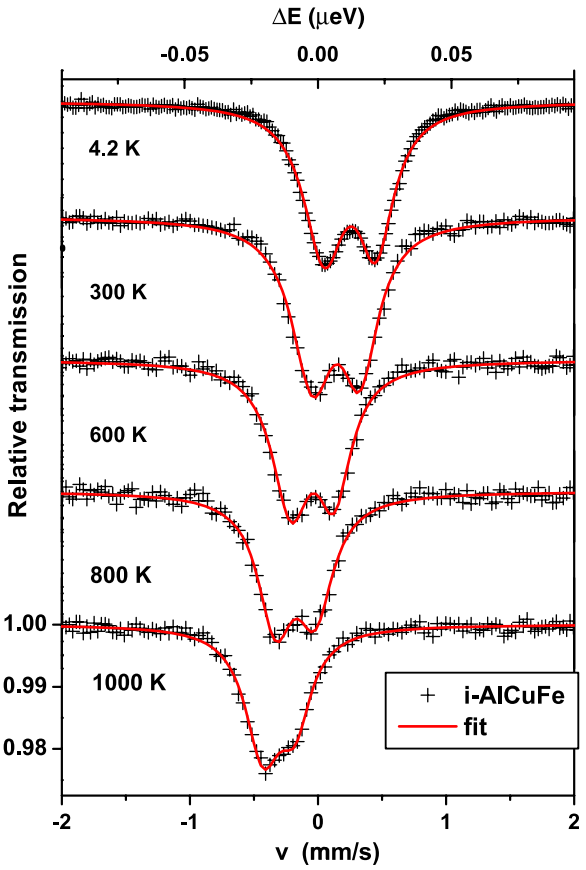

Figure 1. Temperature evolution of the Mössbauer spectra of the natural Fe i-$Al_{62}Cu_{25.5}Fe_{12.5}$. Notice the scale at the top giving the energy shift in μeV as compared to the Doppler velocity given at the bottom in mm s^{-1}. The relative absorption scale, given only for the spectrum at 1000 K, is identical for all spectra.

The spectra were fitted using the method discussed in [47]. The distributions of the centre shift δ and quadrupole splitting Δ have been approximated using a Gaussian form. The hyperfine parameters deduced from the fits are the average centre shift $\langle\delta\rangle$ (always reported referenced to bcc Fe at room temperature), the average quadrupole splitting $\langle\Delta\rangle$, the measured linewidth Γ (FWHM) and the total resonant area a which is proportional to the L–M recoilless fraction $f(T)$ (see the appendix). When only phonons are present, the temperature dependence of $\langle\delta\rangle(T)$ and $f(T)$ can be obtained

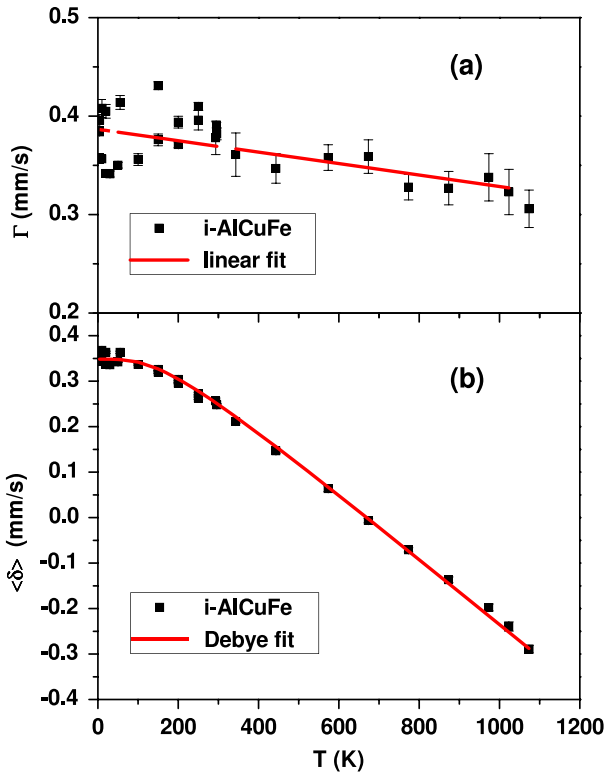

Figure 2. Mössbauer parameters of the natural Fe i-$Al_{62}Cu_{25.5}Fe_{12.5}$ in the temperature range (4.2, 1070 K). (a) The linewidth Γ (FWHM) including a linear fit. (b) The average centre shift $\langle\delta\rangle$ including a fit using the Debye model.

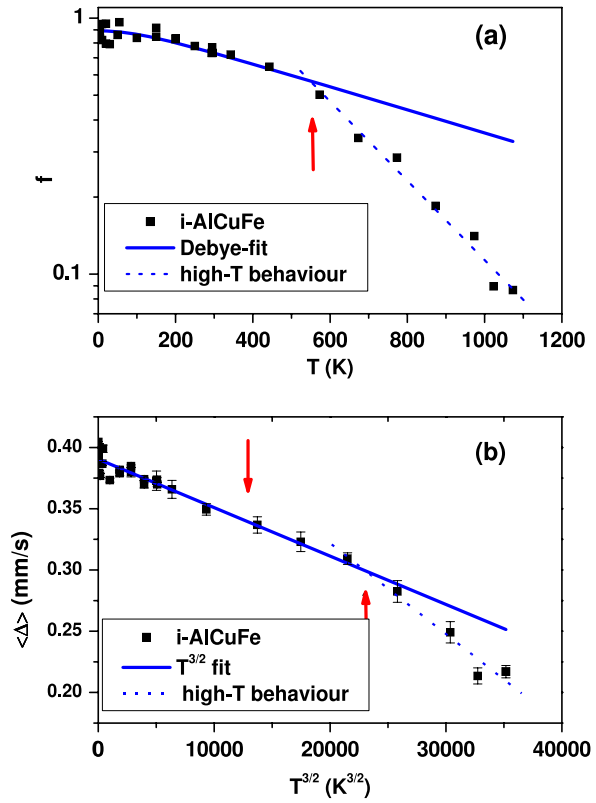

Figure 3. Mössbauer parameters of the natural Fe i-$Al_{62}Cu_{25.5}Fe_{12.5}$ in the temperature range (4.2, 1070 K). (a) The L–M recoilless fraction $f(T)$ on a log scale. The solid line is a fit to the Debye model in the range (4.2, 550 K). Above 550 K, marked by an arrow, there is a change in slope of the measured logarithm of $f(T)$. (b) Average quadrupole splitting $\langle\Delta\rangle$ as a function of $T^{3/2}$. The solid line is a linear in $T^{3/2}$ fit to the data up to 800 K. At this temperature, shown by the rightmost arrow, there is a change in measured slope. An arrow is also given at 550 K. In (a) and (b), the dotted line at high T is only a guide for the eye.

(see the appendix) from the Fe partial vibrational density of states (DOS) $g_{Fe}(\omega)$. The latter can be taken from measurements or from a Debye model.

3.1.2. Natural iron i-$Al_{62}Cu_{25.5}Fe_{12.5}$. The linewidth Γ decreases slightly with temperature: figure 2(a) with a roughly linear evolution. The average centre shift $\langle\delta\rangle$ is shown as the solid points in figure 2(b). A simple Debye model (see the appendix), given as the solid line in figure 2(b), adequately fits the data over the whole investigated temperature range (4.2, 1070 K). The Debye temperature is found equal to 580 ± 6 K. The small error bar is actually artificial: only the low temperature curvature contributes to the fit to Θ_D. The most important information deduced from this fit is that the sample did not degrade and no crystallographic phase change occurred on heating in the Mössbauer experiments, confirming the results of section 2.2. In the case of a phase change in the sample there would be a shift in $\langle\delta\rangle$ at the transition temperature reflecting changes in the chemical isomer shift $\langle\delta_0\rangle$. The differences are large enough to be distinguished. In [50] we published room temperature values for $\langle\delta\rangle$ and $\langle\Delta\rangle$ for this QC phase as well as the surrounding non-QC phases in the Al–Cu–Fe phase diagram.

The temperature dependence of $f(T)$ is shown as the solid points in figure 3(a) on a log scale. As shown in the appendix (see equations (A.1) and (A.5)), in the harmonic (phonon) approximation, the high temperature limit of the logarithm of $f(T)$ is always linear and extrapolates back to $f(0) = 1$. This property has been used here to normalize the measured recoilless area $a(T)$ to obtain the recoilless fraction $f(T)$ using $a(T)$ below the anomalous break in slope (discussed below). The same normalization was found by fitting with a Debye model (below).

Below about 550 K temperature and down to 4.2 K the results could be fitted with a Debye model (see the appendix) shown as a solid line in figure 3(a). The obtained Debye temperature, denoted Θ_D, is equal to 550 ± 50 K. In addition, we can also independently calculate $f(T)$ using the measured Fe partial vibrational DOS $g_{Fe}(\omega)$ which we published previously [41, 42]. This yields results indistinguishable from the Debye result, even though the measured iron partial $g_{Fe}(\omega)$ does deviate from the Debye model although less so than the copper partial or aluminium partial vibrational DOS [51, 52]. We see from equations (A.1)–(A.3) that $g(\omega)$ is the integration kernel for $f(T)$, so that most of the fine structure of $g_{Fe}(\omega)$ has little effect on $f(T)$.

However, there is an abrupt change in slope of the experimental logarithm of $f(T)$ near 550 K. Above this temperature, the measured L–M recoilless fraction is smaller than the predictions based on phonons. This deviation

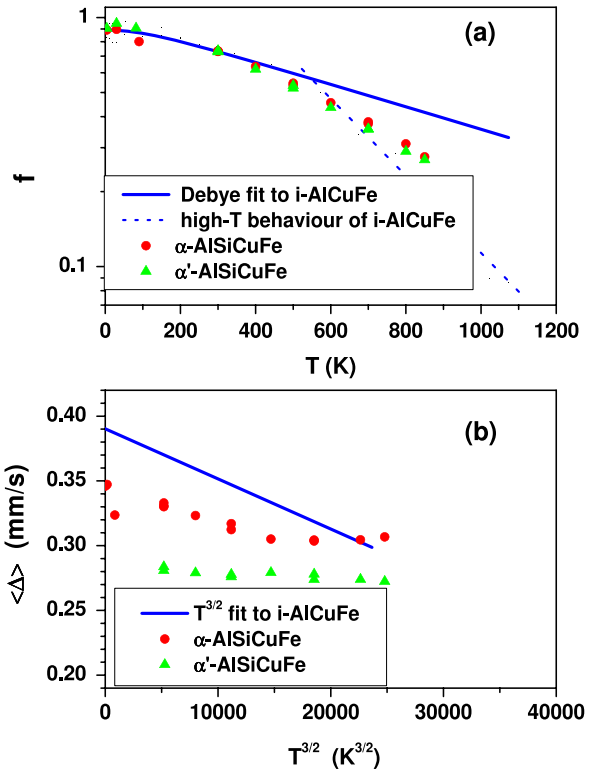

Figure 4. Mössbauer parameters of the 1/1 approximants α-$Al_{55}Si_7Cu_{25.5}Fe_{12.5}$ and α'-$Al_{76.7}Si_7Cu_{3.8}Fe_{17.5}$ in the temperature range (4.2, 850 K). (a) The L–M recoilless fraction $f(T)$ on a log scale. The solid and dotted lines are the same as in figure 3(a) for the i-AlCuFe sample. Both cubic phases display the same anomaly at about 550 K, but weaker than the i-phase. (b) The average quadrupole splitting $\langle\Delta\rangle$ as a function of $T^{3/2}$. The solid line is the same as in figure 3(b) for the i-AlCuFe sample.

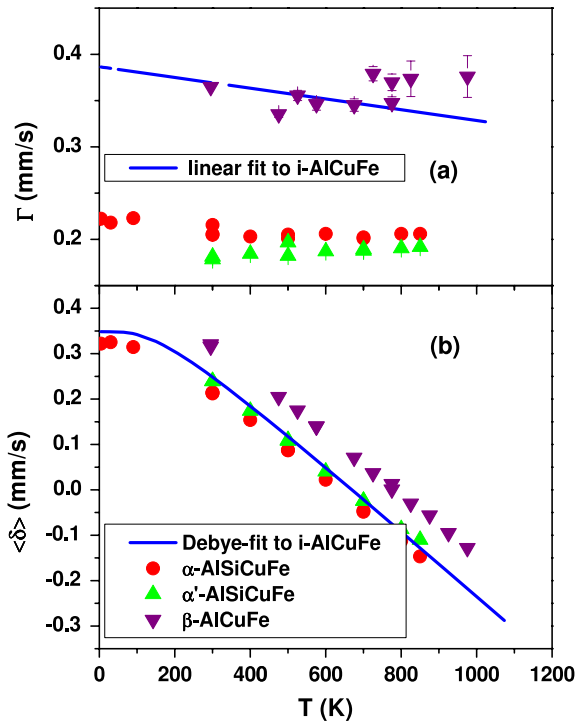

Figure 5. Mössbauer parameters of the 1/1 approximants α-$Al_{55}Si_7Cu_{25.5}Fe_{12.5}$ and α'-$Al_{76.7}Si_7Cu_{3.8}Fe_{17.5}$ as well as the β-$Al_{52}Cu_{35}Fe_{13}$ phase. (a) The linewidth Γ (FWHM). (b) The average centre shift $\langle\delta\rangle$. The solid lines are the same as in figures 2(a) and (b) for i-AlCuFe.

increases with increasing T. The dotted line for the high temperature region and the arrow at 550 K in figure 3(a) are only guides for the eye and the line will be used to compare results on other samples. The missing recoilless fraction will be shown below in section 3.2 to be associated with the presence of a broad quasielastic component (and thus counted here in the background counting rate).

$\langle\Delta\rangle$ is given in figure 3(b). From 4.2 K up to 800 K, $\langle\Delta\rangle$ decreases with temperature, obeying roughly $\langle\Delta\rangle(T) = \langle\Delta_0\rangle(1 - BT^{3/2})$, with $\langle\Delta_0\rangle = 0.39\text{mm s}^{-1}$ and $B = 10^{-5}$ K$^{-3/2}$. This behaviour is found in almost all non-cubic metals, with similar B values [53–55]. Stadnik *et al* [48, 49] also found this dependence in several QCs and approximants studied between 4.2 and 473 K.

Since this 'usual' dependence is not the subject addressed here, this will not be further discussed and the $T^{3/2}$ power law will be taken as the *expected* behaviour at all temperatures, as will be confirmed on the B2 phase presented in section 3.1.4. For the QC i-AlCuFe phase (figure 3(b)), this is no longer found for temperatures above about 800 K, the average $\langle\Delta\rangle$ decreasing much faster than expected. The dotted line in figure 3(b) is a guide for the eye and represents the high T behaviour. What is important is that this deviation from $T^{3/2}$ occurs at a temperature definitely *above* that of the anomaly in $f(T)$ which is at about 550 K.

3.1.3. Cubic 1/1 approximants α-$Al_{55}Si_7Cu_{25.5}Fe_{12.5}$ and α'-$Al_{76.7}Si_7Cu_{3.8}Fe_{17.5}$. Figure 4(a) shows the recoilless fraction $f(T)$ (again, on a log scale) up to 850 K for the two 1/1 samples compared to the results for the i-phase. The solid curve is the Debye fit from the i-AlCuFe phase. The data for α-$Al_{55}Si_7Cu_{25.5}Fe_{12.5}$ and α'-$Al_{76.7}Si_7Cu_{3.8}Fe_{17.5}$ were normalized to this curve in the range (4.2, 550 K) by shifting. This well accounts for the temperature dependence of $f(T)$ in the two 1/1 approximants up to about 550 K, which indicates similar Debye temperatures in the 1/1 phases and in the i-phase. Above 550 K, for the two 1/1 samples, the measured $f(T)$ value is smaller than the extrapolation of the Debye fit. This effect is qualitatively the same as that observed in the i-phase but the amplitude of the deviations is slightly reduced in the 1/1 approximants.

In figure 4(b) the results for $\langle\Delta\rangle$ are shown, again compared with those for the i-phase given as a solid line. In these cubic phases, $\langle\Delta\rangle$ is smaller and shows a weaker temperature dependence in agreement with the results of [48] between 4.2 and 473 K. In figure 5 the results for Γ in (a) and for $\langle\delta\rangle$ in (b) are shown, again compared to the i-AlCuFe results shown as solid lines, the same as in figure 3. As for $\langle\Delta\rangle$, Γ is smaller and less temperature-dependent than for the i-phase. Note that the restricted temperature range imposed by the lack of stability of the 1/1 approximants above 850 K did not allow us to look for the existence of an anomaly in the temperature dependence of the average EFG splitting such as that found in the i-AlCuFe.

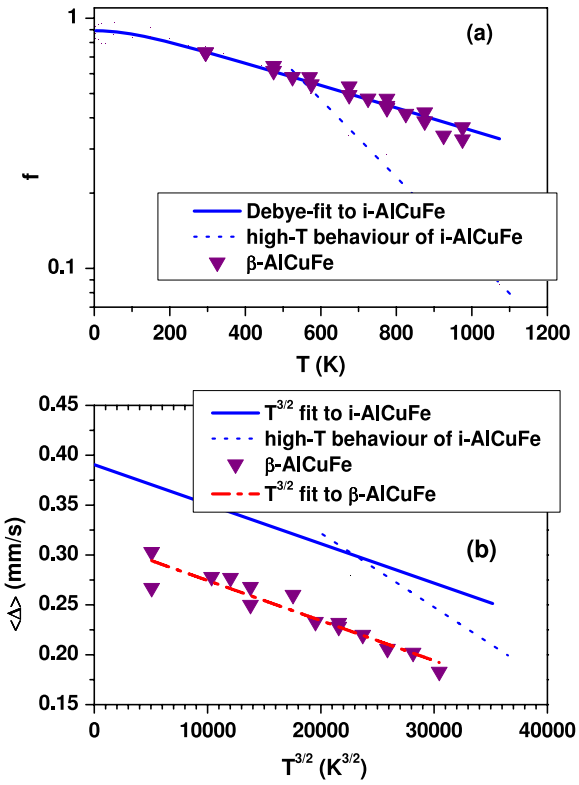

Figure 6. Mössbauer parameters of the β-$Al_{52}Cu_{35}Fe_{13}$ phase from room temperature up to 975 K. (a) The L–M recoilless fraction $f(T)$ on a log scale. The solid and dotted lines are the same as in figure 3(a) for i-AlCuFe. (b) The average quadrupole splitting $\langle\Delta\rangle$ as a function of $T^{3/2}$. Here again the solid and dotted lines are the same as figure 3(b) for i-AlCuFe. The dashed–dotted line is a linear fit to $T^{3/2}$ of the data for the β-phase.

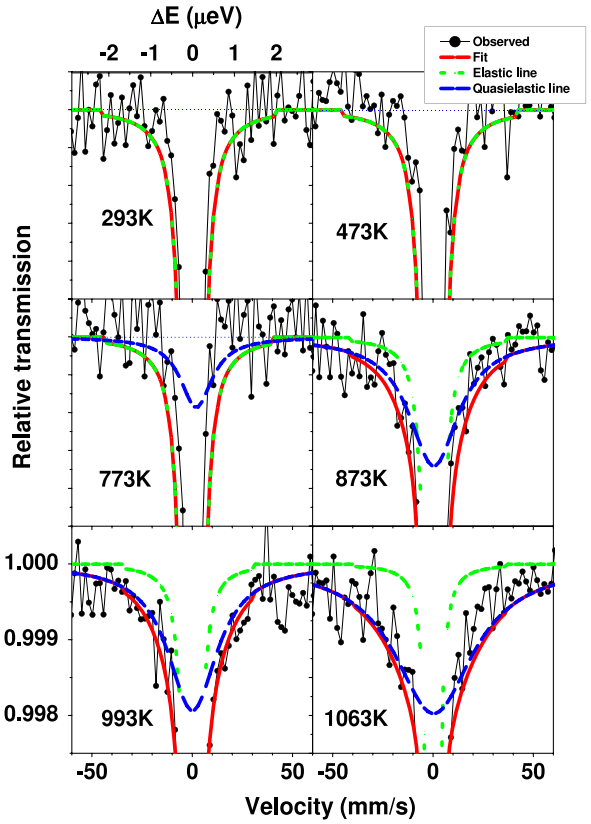

Figure 7. Mössbauer spectra for the ^{57}Fe-enriched i-$Al_{62}Cu_{25.5}Fe_{12.5}$ sample taken at high Doppler velocities for several temperatures from 293 K up to 1063 K. The dotted lines give the elastic contribution and the dashed lines (at 773 K and above) the quasielastic one, their sum (fit) being shown as solid lines. Notice the scale at the top giving the energy shift in μeV as compared to the Doppler velocity given at the bottom in mm s^{-1}.

3.1.4. β-$Al_{52}Cu_{35}Fe_{13}$. The temperature dependence of $f(T)$ in the B2-type β-phase is compared to the results from the i-phase in figure 6(a) where again we show the i-phase simply as the solid and dotted lines. It is apparent that for the β-phase there is *no* anomaly in $f(T)$. In fact, $f(T)$ follows the Debye model of the i-phase with about the same Debye temperature up to 975 K, the maximum temperature of this study. Figure 6(b) shows the results for $\langle\Delta\rangle$. The 'usual' $T^{3/2}$ behaviour is observed up to 975 K. Hence the anomaly detected in the i-phase results above 800 K does not occur in the β-phase. The line broadening Γ is found to *increase* slightly with T rather than decrease, as was the case for the i-phase sample: see figure 5(a). The centre shift $\langle\delta\rangle$ for β compared to the Debye fit to the i-phase is shown in figure 5(b). The shift seen between the i- and β-phase is due to the difference in the average chemical isomer shift between these two phases.

3.2. High velocity Mössbauer results on the ^{57}Fe-enriched i-$Al_{62}Cu_{25.5}Fe_{12.5}$

We now return to the i-phase. In order to investigate the origin of the loss of recoilless fraction observed in the natural Fe sample, we performed a series of Mössbauer experiments on several ^{57}Fe-enriched i-AlCuFe absorbers, using a much wider range of Doppler velocities ($\pm$100 mm s^{-1}). Figure 7 shows a series of spectra taken at increasing temperatures. Note that, at these Doppler velocities, the central elastic part of the spectrum (contained in $\pm$1 mm s^{-1}: see figure 1) is reduced to a very sharp line. As in the low Doppler velocity Mössbauer spectra, the data are normalized to the background counts. We show in the figure a highly expanded scale of the relative counts. The wings of the elastic line (evaluated as explained below) are shown as the dotted line. At 773 K and above, an additional broad contribution is clearly observed. This is shown in the figure as the dashed quasielastic line. Here we describe how we extract this QE signal.

The subspectra labelled elastic in figure 7 have been deduced from spectra measured at the same T at low Doppler velocity ($\pm$2 mm s^{-1}) on the *same* absorber. The high velocity spectra were fitted by adding a Lorentzian quasielastic line to this elastic subspectrum. The fitted parameters were the intensity of the elastic component, the area A_{QE} and the width Γ_{QE} (FWHM above the natural width) of the QE component. In view of the broad width of the QE signal, no quadrupolar splitting has to be introduced for this component. Note that the inelastic scattering due to phonons is spread out over a much wider energy range than investigated in these high velocity experiments and simply adds to the flat background.

A_{QE} and Γ_{QE} are shown in figure 8. Both increase with increasing temperature. At 1063 K, Γ_{QE} equals

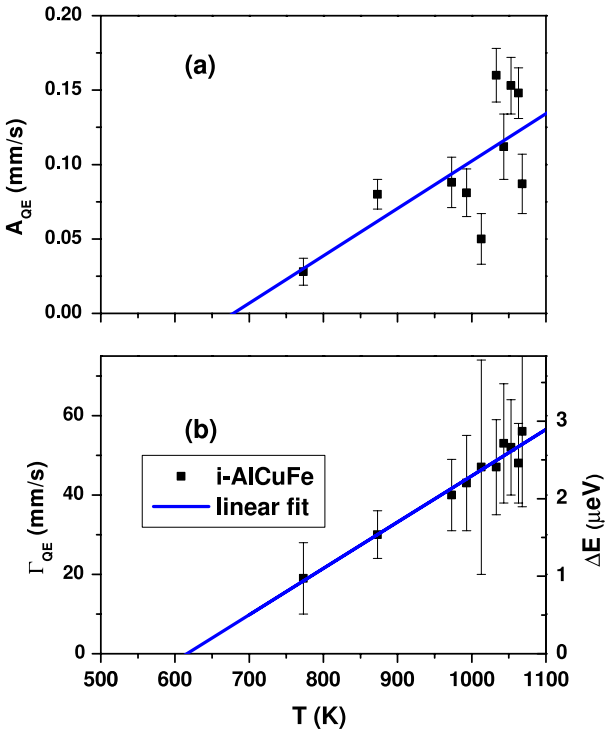

Figure 8. Parameters of the quasielastic component of the Mössbauer spectra for the ^{57}Fe enriched i-$Al_{62}Cu_{25.5}Fe_{12.5}$ as a function of temperature up to 1063 K. (a) The area $A_{QE}(T)$. (b) The linewidth $\Gamma_{QE}(T)$ (FWHM). The right-hand scale gives the equivalent energy. The solid lines in (a) and (b) are only guides for the eye.

56 ± 10 mm s^{-1}, i.e. 2.7 ± 0.5 μeV. This value is not far from that reported (4 μeV FWHM) in [36] at 1060 K for data with a lower signal-to-noise ratio on a similar i-AlCuFe sample.

In conclusion, the appearance of the quasielastic component and its increase in intensity with increasing temperature up to 1063 K are clearly correlated with the anomalous decrease in $f(T)$ above 550 K reported in section 3.1.2 for the natural Fe i-AlCuFe sample. In the low velocity spectra the quasielastic component merges into the energy-independent background counting rate. The area of the elastic and quasielastic components should obey a sum rule, their sum being the value of $f(T)$ predicted from the phonon spectrum. However, the strong nonlinear absorption in the enriched samples precludes a rigorous test of this expectation. Nevertheless qualitative arguments can be given.

Let us first note that near 1000 K the QE line is about a factor of 100 times broader than the elastic one. Then, for equal areas (intensity) it would be 100 times less deep. This makes a strong QE signal appear to be very weak. As explained above, in order to measure the QE contribution we have used samples enriched in ^{57}Fe, and a large velocity range.

This creates difficulties in analysing simultaneously the QE signal and the narrow elastic part of the spectrum. A rigorous test of the sum rule between the elastic and the quasielastic contributions would entail a fit of both components in one spectrum, and then a calibration (converting measured area in mm s^{-1} to recoilless fraction f for both contributions). In the case of a large Mössbauer thickness parameter t_{ab}, this should entail using the proper transmission integral to properly account for spectral distortion of mainly the central, elastic, component. This is made difficult by the large velocity interval pro channel as compared to the variation in absorption pro channel at the centre (leading to averaging effects), rendering the transmission integral fit unstable.

3.3. Neutron scattering results on the natural iron and ^{57}Fe-enriched i-$Al_{62}Cu_{25.5}Fe_{12.5}$

Neutron spectra were measured at 600 and 1050 K. The raw data were first corrected for detector efficiency, sample mass, absorption and removal of the sample holder contribution in order to obtain the scattered intensity as a function of the neutron energy transfer $\Delta E = \hbar\omega$. Spectra can be produced either by summing over all detectors, or by grouping them in groups of two. The latter are proportional to the scattering function $S(Q, \hbar\omega)$. Data in the high-Q range were affected by strong Bragg reflections (whose intensities changed between the two samples). The affected detectors were not used in the further analysis of either sample. In addition, the total intensity at the first two detectors was anomalously high, so the lowest-Q region was also deleted (0.02–0.28 Å^{-1}). Therefore we report only on data with Q values of 0.49, 0.71, 0.92, 1.11, 1.29, 1.46 and 1.66 Å^{-1}.

The phonon inelastic scattering is spread out over a range of several meV and thus appears as a flat background in our energy range (± 15 μeV). Hence, to analyse the spectra we use a model which is the sum of a constant background, a delta function (accounting for the elastic contribution) and an eventual quasielastic (QE) contribution assumed to be a single Lorentzian. Then the model is convoluted with the experimental resolution function.

The 600 K spectra summed over all Q values could be satisfactorily explained for both samples by the sum of the elastic contribution and a flat background. Hence no QE signal could be detected at 600 K. The analysis of the 1050 K spectra also summed over all Q for the natural Fe i-AlCuFe sample reveals the presence of an additional small QE signal. The QE signal being much smaller than the elastic contribution, its accurate separation from the wings of the elastic peak, enlarged by the finite resolution, is difficult. Hence we have analysed our data using a difference method, along similar lines as Coddens *et al* [32]. Difference spectra were built by subtracting the spectrum at 600 K from that for 1050 K at each Q value. The elastic intensity decreases with increasing temperature due to atomic vibrations. At 1050 K, atomic jumps will contribute to an *additional* decrease of the elastic contribution, as is the case for the L–M recoilless fraction in Mössbauer experiments. Therefore the elastic contribution will always appear *negative* in the difference spectra. Any quasielastic contribution, present at 1050 K and negligible or absent at 600 K, will appear *positive*. Note that the validity of this treatment depends on the separability of the elastic and quasielastic terms and assumes that the elastic component remains sharp (resolution-limited). It would not apply to a situation where the entire elastic peak becomes quasielastic at high temperature, as is the case when diffusion of all the

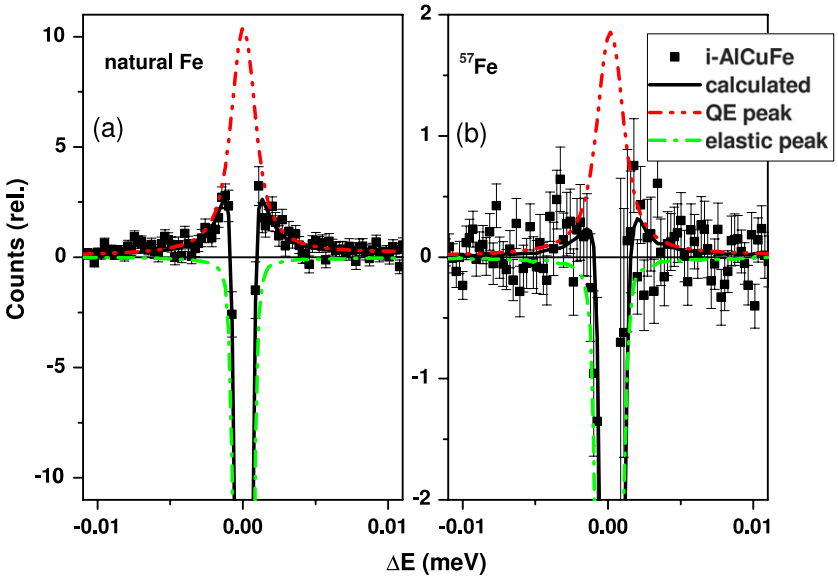

Figure 9. Neutron spectra summed over all Q values from 0.49 to 1.66 Å^{-1} (a) for the natural Fe i-AlCuFe phase and (b) for the ^{57}Fe-enriched one. Shown is the difference spectrum from that at 1050 K minus that at 600 K. The dashed–dotted (negative-going) line accounts for the elastic component. The positive-going dashed–double-dotted line represents the quasielastic contribution. The solid line is the sum of these. Note the difference in scales in (a) and (b).

chemical species present in the material occurs [24]. The resulting difference spectra (summed over all Q values) are shown in figure 9(a) for the natural Fe and in (b) for the ^{57}Fe-enriched samples. As expected, they exhibit a strong negative-going central region, due to the elastic contribution.

Let us first analyse the natural Fe sample. A broader positive-going signal, centred at zero energy, is clearly visible in figure 9(a), revealing the existence of a QE component. The difference spectrum was fitted including a (Lorentzian) quasielastic signal. The width of the QE line (FWHM) is 1.5 ± 1 μeV, smaller than the value reported by Coddens *et al* of 4 ± 1 μeV in [32]. This difference probably comes from slight differences in modelling the resolution function, which affect the separation between the wings of the elastic contribution and the QE signal. This analysis confirms unambiguously the existence of a quasielastic signal in the natural Fe i-AlCuFe at 1050 K. Its Q dependence could not be studied because the spectra at fixed Q did not have a sufficient signal-to-noise ratio.

For the ^{57}Fe-enriched i-AlCuFe sample, the difference spectrum is presented in figure 9(b). It is apparent that any quasielastic contribution is much smaller than for the natural Fe sample. Fixing the width of the QE signal in the ^{57}Fe-enriched sample to the value found in the natural Fe sample, the ratio of the area between the ^{57}Fe-enriched and natural Fe was found to be about 0.2. From the work of [32] we already know that the intensity of the quasielastic component is insensitive to the Cu scattering cross section. From the composition-weighted scattering cross sections [56] presented in table 1, we see that the ratio of the Al + Fe cross sections is 0.44, while the ratio of the ^{57}Fe to natural Fe cross section is about 0.086. We can therefore conclude that, although Al contributes, Fe dynamics is the dominating contribution to the QE line detected in NS. This conclusion is coherent with the fact that the QE lines detected in high velocity MS and in NS have similar linewidths.

Table 1. Composition-weighted neutron scattering (coherent plus incoherent [56]) cross sections in barns for each element in the two i-$Al_{62}Cu_{25.5}Fe_{12.5}$ samples. The total scattering cross section σ_s is given in the last column.

Fe	σ_s^{Al}	σ_s^{Cu}	σ_s^{Fe}	σ_s
Natural	0.931(2)	2.048(8)	1.452(12)	4.27
^{57}Fe	0.931(2)	2.048(8)	0.125(37)	2.99

4. Discussion

4.1. Summary of literature results

In addition to previous diffuse scattering and neutron time-of-flight and quasielastic scattering results, there is other clear evidence that the atomic dynamics in QCs of the i-AlPdMn family is anomalous at high temperatures. Edagawa *et al* [57, 58] and Shulyatev *et al* [59] have presented high temperature specific heat data on several such QCs and shown that they deviate very strongly from the Dulong–Petit law 3 k_B/atom. For i-AlPdMn the specific heat increases above 3 k_B for temperatures above 700 K and reaches 4.7 k_B at 1080 K. In contrast, the deviation of a crystal approximant Al-Pd-Fe is much smaller, it is about 3.6 k_B at 1080 K. Edagawa *et al* discuss the origin of the large deviations of the quasicrystals from Dulong–Petit's value in light of the thermal excitation of phasons. Shulyatev *et al* present similar data for i-AlCuFe and decagonal d-AlNiCo.

Previous studies of the L–M recoilless fraction $f(T)$ have been presented by Janot *et al* [34] for i-$Al_{62}Cu_{25.5}Fe_{12.5}$ and de Araújo *et al* [35] for i-$Al_{63.5}Cu_{24}Fe_{12.5}$ from 293 K up to 1076 K. These $f(T)$ data, shifted on a logarithmic scale so that the linear part from 300 to about 550 K extrapolates to $f = 1$ at zero temperature (see the appendix), are compared

to our results in figure 10(a), shown as the solid and dotted lines. A good superposition is obtained. The Debye fit with $\Theta_D = 550$ K, found for our sample in section 3.1.2, accounts well for the behaviour of the two other samples in the range (300, 550 K), indicating similar Debye temperatures in the three samples, as expected from their similar compositions. Above 550 K, in all samples, the L–M fraction is smaller than expected from the Debye model.

To our knowledge an anomaly in the temperature dependence of the average quadrupole splitting has not been mentioned in the literature so far. However, de Araújo *et al* [35] gave data for the average quadrupole splitting $\langle\Delta\rangle$ as a function of T in the range (293, 1076 K). In figure 10(b) we report their data as a function of $T^{3/2}$, compared to ours. Note that in [35] $\langle\Delta\rangle$ was evaluated using a distribution algorithm, which weights the higher splittings more than our single enlarged doublet model does, so the results obtained for $\langle\Delta\rangle$ are consistently about 10% larger than ours. But a comparison in temperature is all we are interested in here. A $T^{3/2}$ law accounts for the data of de Araújo *et al* up to about 800 K. Above this, there might be a change in slope, and if we delete their data point at 1024 K then we indeed obtain a slope compatible with the one observed in our sample. Note that de Araújo *et al* gave another analysis of their results, concentrating on their two high temperature points and proposing a structural transition to a perfect QC phase above 1000 K. From this comparison of all available low velocity Mössbauer results, we can conclude that all i-AlCuFe samples exhibit the same behaviour, although some of the effects had remained unnoticed in the literature.

In the two 1/1 approximants studied here, a loss in $f(T)$ occurs above 550 K, revealing the same kind of Fe dynamics as in the i-phase but the effect is smaller. These results should bring some hints for identifying the hopping sites in the QC structure, taking advantage of the now well-known chemical decoration of the 1/1 phases [43] and its link with the i-phase [60]. For the B2 β-$Al_{52}Cu_{35}Fe_{13}$ phase we have established in the present work that no anomalous Fe dynamics (other than phonons) occurs, contrary to the case of the i-phase and approximant phases. Hence no Fe jumps are detected in the B2 phase.

The only related study in the literature is that of Coddens *et al* [32] who have presented some results on AlCuFe approximants using QE neutron scattering. In the 100 μeV energy range where Cu jumps are detected in i-AlCuFe, the rhombohedral AlCuFe phase, a high order ($p/q = 3/2$) approximant [40], behaves exactly like the i-phase. In addition, no Cu jumps could be detected in the 1/1α-$Al_{55}Si_7Cu_{25.5}Fe_{12.5}$ phase at 953 K and in the B2-type β-$Al_{50}Cu_{25}Fe_{25}$ phase at 1063 K in this energy range.

Dahlborg *et al* [61] have detected Cu and Ni jumps with energy ranges close to those in QCs in a crystalline $Al_{50}Cu_{35}Ni_{15}$ phase at 1193 K and concluded that rapid atomic jumps are likely to occur in any metallic alloy at high temperature and are not a specific property of quasicrystals. This statement has led to some controversy in the literature [62, 63]. Clearly the present results show that reality is much more complex. The Fe jumps observed in

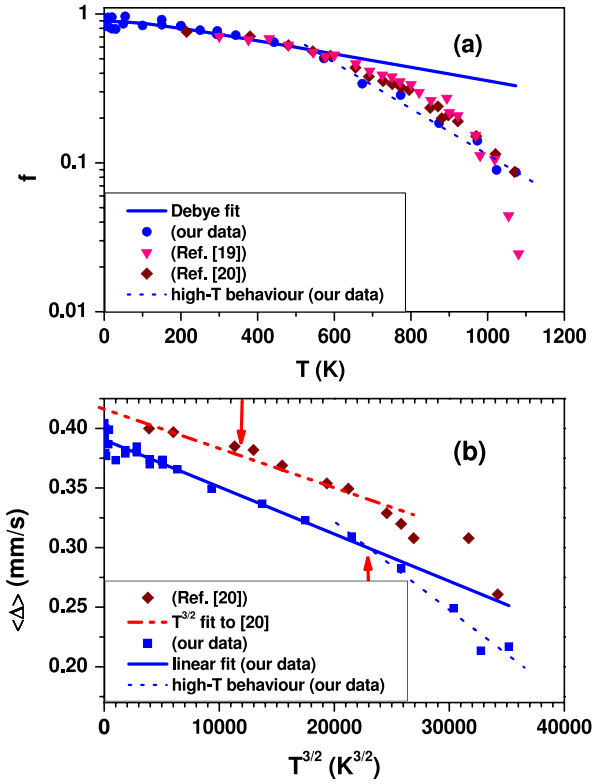

Figure 10. Our data for $f(T)$ and $\langle\Delta\rangle$ in i-AlCuFe compared to literature results. (a) The recoilless fraction $f(T)$. The solid and dotted lines are the same as in figure 3(a) for our i-$Al_{62}Cu_{25.5}Fe_{12.5}$. Shown as well are the literature data for the same composition i-phase [34] and for i-$Al_{63.5}Cu_{24}Fe_{12.5}$ [35]. (b) The average quadrupole splitting $\langle\Delta\rangle$ as a function of $T^{3/2}$. The solid line is a $T^{3/2}$ fit to our data up to 800 K, shown by the upper arrow. Shown as well are the literature data for i-$Al_{63.5}Cu_{24}Fe_{12.5}$ [35]. The dashed–double-dotted line is a fit to the data of [35] up to 800 K. The dotted lines from figure 3 for (a) and (b) are only guides for the eye.

the QC do not exist in the B2 β-$Al_{52}Cu_{35}Fe_{13}$ phase. We will confine ourselves to a few comments. It is well known, since the work of Vogl [27, 29, 64], that fast local hopping is characteristic of some crystalline systems in which the jumping atom is connected to a cage of nearby possible sites. Hence certainly all hopping processes are not linked with phasons in quasicrystals. It will be the case only if they are related to a perpendicular space or amenable to a Penrose tile description. This could indeed be the case in the $Al_{50}Cu_{35}Ni_{15}$ phase studied in [61] since its B2-based structure (designated in the literature as a tau-phase) is particular and exhibits a quasiperiodic vacancy order [65].

4.2. Modelling results

In MS, as in NS, one actually measures the incoherent dynamical structure factor $S_{inc}(\vec{Q}, \omega)$, related to the self-correlation function $G_s(\vec{R}, t)$ giving the probability to find an atom at $\vec{R}$ at time t which was at the origin at time zero. For NS, the wavevector $\vec{Q}$ varies whereas for MS it is the wavevector of the Mössbauer radiation and thus fixed ($Q = 7.29$ Å^{-1} for the 14.4 keV radiation of ^{57}Fe).

In the following we will only treat the case of MS but the same conclusions could be applied to NS. For neutron scattering, a problem arises that the incoherent neutron cross section is actually much smaller than the coherent one (see table 1). When the momentum transfer is large enough, inelastic scattering is not sensitive to structural correlations (which lead to diffraction) so that the incoherent approximation [66–68] is applicable, where we treat the scattering as if it were incoherent, but use the total scattering cross section. This is what Coddens *et al* [30] found in i-AlCuFe.

Considering atomic jumps in a restricted cage, a separation into very fast thermal vibrations and slower jump rates within the cage is usually possible. Petry and Vogl [28] have given the solution for an octahedron cage (ignoring the electric field gradient: see later). The contribution of localized atomic jumps to the MS spectrum consists of a sum of different QE Lorentz lines with FWHM of $\Gamma_j = \Gamma_0 + 4j\gamma_j$ where Γ_0 is the natural linewidth of the nuclear transition. The index j runs from 0 (centre position) over all allowed jump vectors $\vec{R}_j$ with jumping rate $1/\tau_j$ given by $\gamma_j/\hbar$. The $j = 0$ term is the elastic line (with unchanged linewidth Γ_0) but intensity reduced by the sum of all QE contributions. Thus, provided that $4\gamma_j$ is not negligible with respect to Γ_0, the MS spectrum consists of QE lines coexisting with an elastic one. In the limit of equal partition over the states (high temperature limit) this leads to a 'jump Debye–Waller factor' for the elastic line f_{Jump} given by $f_{\text{Jump}} = |(1/N)\sum_j \exp(-\mathrm{i}\vec{Q}\cdot\vec{R}_j)|^2$. As a last comment we mention that the factor of four in the above depends on the geometry of the model and different models give different factors.

In summary, localized atomic jumps lead to the coexistence of quasielastic and elastic contributions, the intensities of which are related by a sum rule. The physical reason is that, in the case of cage motion, the atom has a finite probability to return back to its original position even at long times.

The situation encountered in the case of the long ranged motions involved in atomic diffusion is completely different. The correlation between successive jumps is then much smaller. As a consequence, the unbroadened line ($j = 0$) disappears and the MS (or NS) spectrum consists of a single QE line (or perhaps a sum over QE lines). Its integrated intensity follows the behaviour expected for thermal vibrations and hence there is no anomaly in the measured $f(T)$. Its width Γ_{QE} (FWHM above the natural width) increases with increasing temperature. It can be related to the residence time as $\tau = 2\hbar/\Gamma_{\text{QE}}$ (to within a model-dependent factor) and hence to the diffusion constant D using $D = R^2F/6\tau$ [69], where R is the jump distance and F is the correlation factor: the fraction of jumps not leading back to the original position.

In both the i-AlCuFe QC and the 1/1 cubic approximants, we observe an elastic line which does not broaden at high temperatures but shows a loss of recoilless fraction f above about 550 K. In the i-phase, we could establish that this loss is correlated with the appearance of a QE component. Although the existence of a sum rule could not be quantitatively proven (see section 3.2), one can note that the intensity of the QE line and the difference between the calculated f value for thermal vibrations and the measured one exhibit the same qualitative temperature evolution in the temperature range (773, 1070 K), where the QE line could be detected. They both steadily increase with temperature.

Based on these observations it is reasonable to assume that the QE line, although too weak to be detected below 773 K, appears at about 550 K, which is the temperature at which f exhibits its anomalous decrease. These results certainly suggest that we are observing a type of cage motion for the Fe atoms rather than diffusion. It is then consistent to interpret these as phason flips on a quasiperiodic or approximant lattice. In the following we will give a simple model of the Fe atomic jumps as such tiling flips which do correspond to experimental results, including the temperature dependence of the quadrupole splitting. But before presenting this interpretation, we consider two alternatives, namely diffusive motion of the Fe, or localized shell vibrations.

One could propose the coexistence of two kinds of Fe atoms, one only vibrating around equilibrium atomic positions and responsible for the elastic component and the other one diffusing and responsible for the QE line. Although it would be difficult to explain why the proportion of diffusing Fe atoms should increase with temperature in this model, let us consider it further and try to interpret the width of the QE line as resulting from long range diffusion. From the Γ_{QE} value measured at 1000 K ($\sim$2 μeV) one can estimate the residence time (of the order of 660 ps) and hence get an order of magnitude for the diffusion constant D ($\sim 10^{-11}$ m^2 s^{-1}) using $R = 2$ Å and $F = 0.78$ (the value for an fcc lattice).

Although this calculation is not actually applicable (since the atomic motion observed here is not random-walk-like and we do not have an fcc lattice), it does permit a direct comparison to the results of macroscopic diffusion measurements. The latter are definitely smaller. Mehrer [70] has summarized the current literature results. The values of D found for transition metals in pure aluminium lie in the range of 10^{-12} m^2 s^{-1}, and in single-crystal i-AlPdMn (isostructural with i-AlCuFe) in the range of 10^{-16} to 10^{-13} m^2 s^{-1} with diffusion of Fe at the lower end of this range (values given for 1000 K). Clearly the observed QE line is too large to be ascribed to long range diffusion of Fe.

An additional and even stronger argument (not affected by the arbitrary guess of an F value) comes from the analysis of the temperature dependence of Γ_{QE}. We can try to analyse it assuming an activation law (Arrhenius form) $\Gamma_{\text{QE}}(T) = \Gamma_\infty \exp(-E_{\text{A}}/k_{\text{B}}T)$. A satisfactory fit can be obtained with an activation energy E_{A} of 0.25 eV/atom but this value for E_{A} is an order of magnitude lower than that obtained from the macroscopic diffusion measurements. This means that, at temperatures lower than 1000 K, the difference between measured D values and D values estimated from the QE linewidth is even several orders of magnitude larger. Unfortunately, only the two temperatures reported on for the INS experiments were possible due to low counting statistics (the QE neutron scattering experiments of Janot *et al* [34] were with a fixed energy window of 1 μeV).

Another explanation of both the anomalous decrease in the L–M recoilless fraction and neutron elastic scattering

intensity has been proposed in [34] in terms of vibration modes localized on clusters. It seems to us that this interpretation can be discarded for several reasons. First of all, and most importantly, localized vibrations cannot produce a QE line. Other arguments are that, in the case of localized vibrations, there is no energy barrier and so there should be deviations from the behaviour predicted from phonons at all temperatures. This was shown in the work of Maradudin *et al* [71] and experimentally confirmed [72, 73]. Moreover local vibrations should affect the T dependence of the Mössbauer second-order Doppler shift, which is not the case in our work (figure 2(b)) as well as in [35].

Thus the only reasonable interpretation of our results is to assume that Fe atoms are undergoing localized jumps. Then one has to explain why, from 550 to 800 K, Fe jumps occur with no change in EFG splitting, while above 800 K this splitting decreases strongly. There is also an increase in spectra asymmetry (relative intensities between the two lines) with increasing temperature (see an example in figure 1). As an expositional example we will use the work of Litterst *et al* [74, 75] who have calculated the Mössbauer spectrum for Fe atoms hopping between the apices of an octahedron. In this calculation, one assumes that the EFG tensors have the same eigenvalues at each site. For simplicity, cylindrical symmetry is assumed with the principal tensor axis parallel to the vector joining the centre of the octahedron to the site. Two different jumps are possible (figure 11(a)). An axial jump (length $2r$) between two opposite apices (characteristic timescale τ_1) preserves the orientation of the EFG principal axis system since this jump occurs between mirror-related sites. A jump (length $\sqrt{2}r$) between two neighbouring apices (characteristic timescale τ_2) implies a *rotation* of the EFG principal axis. Both kinds of jumps lead to a QE signal which is the signature for cage motion.

For jumps between opposite apices no decrease of the EFG splitting of the central line occurs but for jumps between neighbouring apices, a decrease, and eventual collapse, at very large τ_2 in the effective EFG splitting is obtained, accompanied by a growing asymmetry of the Mössbauer spectra. These effects are driven by the dynamical mixing of the EFG-split nuclear energy levels of the ^{57}Fe excited state. Vogl and co-workers have observed such effects for Fe implanted into α-Zr and into Al [76, 27, 29, 64].

We emphasize here the important point that these model results *do not depend on the specific geometry of an octahedron*. The essence lies in the fluctuations of the hyperfine interactions which may or may not be accompanied by a *rotation* of the principal axis system of the EFG tensor. The point of discussing this model is not to conclude that there are octahedral Fe sites in the QC, but to establish the effect of the rotation of the EFG principal axes on the apparent EFG splitting during an atomic jump, which is model independent.

We therefore conclude that Fe is involved in at least two different local atomic jump processes in i-AlCuFe and that there are at least two different modes of tiling flips (phasons) involving Fe in i-AlCuFe at high temperatures. These two processes can be characterized as, first, a mirror-symmetric tiling flip and, second, a rotational tiling flip

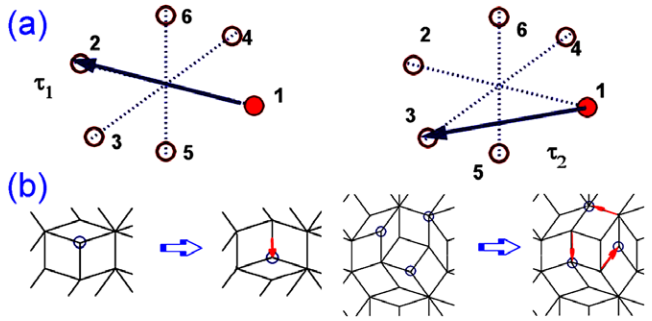

Figure 11. (a) A regular octahedral cage. The Mössbauer atom is assumed to jump between the apices. Two different possible jumps are shown with relaxation times τ_1 (left) and τ_2 (right). (b) The possible types of atomic jumps shown as tile flips on a Penrose quasiperiodic lattice: without (left) and with (right) rotation of the local principal axis of the EFG.

(figure 11(b)). Note that the evidence for two different jumps is the temperature dependence of the EFG. Note that the evidence for two different jumps is the temperature dependence of the EFG: a departure from the $T^{3/2}$ behaviour found below 500 K.

The two different jumps could not be distinguished in the analysis of the QE line. Either they have similar characteristic timescales and hence their QE contributions are mixed or the jump starting above 800 K does not occur in the energy window of the high velocity Mössbauer experiments.

A comment must be made on the $T^{3/2}$ behaviour of the EFG. Our goal is not to discuss its origin in AlCuFe phases. Indeed this behaviour, commonly observed in non-cubic metals [53–55] and previously in some QCs [48, 49], has no well-established theoretical basis. (It has been obtained in hcp-Cd from first-principles calculations [77] and ascribed to the influence of the electronic structure and vibrational DOS on the EFG.) However, it can be used to show the change of regime in the temperature dependence of the EFG at 800 K which occurs in the i-AlCuFe phase but not in the B2 β-$Al_{52}Cu_{35}Fe_{13}$ phase.

5. Conclusions

We have demonstrated the existence of Fe localized jumps in the i-AlCuFe QC and were able to clarify their temperature dependence. Interpreting the temperature dependence of Γ_{QE} in this framework, one can conclude that Fe jumps obey a thermal activation law, with an activation energy E_A of 0.25 eV/atom. This is in strong contrast with the absence of any T dependence observed for the Cu jumps detected so far in i-AlCuFe [30, 32], as well as for atomic jumps observed in i-AlPdMn [31] and in the decagonal d-AlCoNi phase [78]. Hence, whereas the thermal behaviour of the Cu jumps in i-AlCuFe cannot be explained by simple thermal activation of Cu atoms, that of Fe can be.

Despite this vast difference in residence times for Fe and Cu, it is striking to note that for both jumps the intensity of the QE line steadily increases with temperature. Cu jumps are unambiguously observed at 723 K in [30] through the detection of a QE line. It is possible that they start at a lower

temperature but the QE line is then too weak to be detected. In the present work, because of Lamb–Mössbauer recoilless fraction data and their established correlation with the intensity of the QE line, we have a very precise determination of the temperature at which Fe jumps start to occur: 550 K. This pinpoints the starting temperature for Fe jumps due to phasons much better than previous studies and makes comparisons with other experiments possible, as we will now discuss.

It is very interesting to compare our recoilless fraction results with the specific heat data of Edagawa *et al* [79] on i-AlPdMn and d-AlCuCo QCs. They observed an anomalous increase of the constant volume specific heat C_v above 600 K. reaching 5 k_B/atom near 1000 K, far above the classic 3 k_B/atom limit given by the harmonic approximation. Small increases in C_v above 3 k_B/atom near the melting point are expected and usually observed, but the results of [79] are difficult to explain simply on this basis. Something more dramatic is needed, similar to local melting. However, their results do not suggest a phase transition in the sense of a new structure. A depinning of the (frozen) phasons above 600 K is proposed in [79]. Our results are consistent with such an interpretation.

As shown in section 4.2 it is consistent to interpret the two kinds of Fe jumps detected in the i-AlCuFe QC as tiling flips (phasons). However, one should emphasize that the present results demonstrate that a quasiperiodic long range order is not required to generate these local iron jumps. We observed similar, although reduced, effects in the two cubic 1/1 approximants α and α'-AlSiCuFe. Significantly, no local Fe jumps are detected in the simple cubic B2-type β-AlCuFe phase. Hence the existence of local iron jumps must be linked to local environments present, at least partly, both in QCs and approximants.

Going further and trying to identify the Fe sites where jumping (mainly) occurs is a very difficult task. We confine ourselves to a few general remarks:

- The i-AlCuFe QC has a strong chemical order as shown by the models of decoration given in [80], and EXAFS refinement given by Simonet *et al* [60]. This is consistent with the hypothesis of different Fe sites with different environments and hence possibly different jump characteristics. The same remark may explain why Fe and Cu jumps are so different.
- The first Fe jump starting at 550 K does not change the EFG. Thus it preserves the local symmetry. This is actually the simplest type of flip of Penrose tiles and so there are probably several different possibilities in the QC lattice.
- One remarkable feature of the QC model of [80] is the existence of a partially filled icosahedron occupied by Fe atoms. An Fe jump from one vertex of this icosahedron to another provides a likely candidate for the rotational tiling flip observed above 800 K. However, cooperative jumps involving several atoms are possible and, in fact, most probable.
- The 1/1 AlSiCuFe approximants also exhibit a strong chemical order and their chemical decoration is well known (see [43] and references therein). It is closely linked with that of the QC and again there are probably several different possibilities for flips conserving symmetry. Note that no partially filled icosahedron is present in the α' approximant. One is found in the α approximant but is then occupied by Al. Hence, if the symmetry-breaking jumps observed in the QC above 800 K are *only* due to Fe atoms on such an icosahedron, they should not exist in the approximants studied here. Unfortunately this hypothesis cannot be tested since it is not possible to study the approximants at high enough temperature.

Acknowledgments

This research was supported in part by the DFG Priority Programme 'Quasikristalle: Struktur und physikalische Eigenschaften' under project BR862/9. We thank Denis Gratias, Marianne Quiquandon, Virginie Simonet and Gerrit Coddens for many fruitful conversations on this subject and Jürgen Voß for some of the measurements. None of this work would have been possible without the expert sample preparation and collegial cooperation of Yvonne Calvayrac.

Appendix

In this appendix, the temperature dependences of the average centre shift $\langle\delta\rangle$ and recoilless fraction $f(T)$ are given in the case of harmonic lattice vibrations (phonons). The nuclear lifetime of (any) Mössbauer transition is long compared with typical inverse phonon frequencies. Thus the lattice displacement x and associated velocity v can be averaged over many lattice oscillations, so that linear terms in x or v cancel. The recoilless fraction is related to the mean square displacement $\langle x^2\rangle$ of the Fe nucleus in the direction of the Mössbauer radiation [45]. The centre shift δ is the sum of the chemical isomer shift δ_0 and the temperature-dependent second-order Doppler (SOD) shift $\delta_{SOD}(T)$. δ_0 is temperature-independent as long as the sample does not undergo any phase transformation. $\delta_{SOD}(T)$ is related to the mean square velocity of the Fe nuclei $\langle v^2\rangle$ [45]. One has

$$\ln f(T) = -k^2\langle x^2\rangle \qquad \text{and} \qquad \delta_{SOD}(T) = -\frac{\langle v^2\rangle}{2c}. \tag{A.1}$$

k is the magnitude of the wavevector of the Mössbauer radiation ($k = 7.29$ Å^{-1}) and c is the velocity of light. In the harmonic approximation (see [81]), $\langle x^2\rangle$ and $\langle v^2\rangle$ can be expressed as averages over the eigenfrequencies:

$$\langle x^2\rangle = \frac{\hbar}{M}\langle\omega^{-1}\rangle \qquad \text{and} \qquad \langle v^2\rangle = \frac{3\hbar}{M}\langle\omega\rangle. \tag{A.2}$$

M is the mass of the Mössbauer isotope. The different moments $\langle\omega^l\rangle$ can be expressed as integrals over the (atomic-partial) vibrational density of states (DOS) $g(\omega)$, the Bose occupation factor $\bar{n}$ and ω^l:

$$\langle\omega^l\rangle = \int_0^\infty g(\omega)\left(\bar{n} + \tfrac{1}{2}\right)\omega^l\,\mathrm{d}\omega. \tag{A.3}$$

Note that $\ln f(T)$ will weight the lower frequencies and $\delta_{\mathrm{SOD}}(T)$ the higher ones. Both the high temperature and zero temperature limits can be given for $\langle x^2\rangle$ and $\langle v^2\rangle$ as functions of the (temperature-independent) weighted mean frequencies $\widetilde{\omega^n}$ where

$$\widetilde{\omega^n} = \int_0^{\omega_{\mathrm{m}}} g(\omega)\omega^n \,\mathrm{d}\omega. \tag{A.4}$$

ω_{m} is the highest frequency contributing to $g(\omega)$. The high temperature limit is given by a Thirring expansion, convergent for $k_{\mathrm{B}}T > \hbar\omega_{\mathrm{m}}/2$ where we give only the leading terms:

$$\langle x^2\rangle \simeq \frac{kT}{M}\widetilde{\omega^{-2}} \qquad \text{and} \qquad \langle v^2\rangle \simeq \frac{3kT}{M}. \tag{A.5}$$

Both $\langle x^2\rangle$ and $\langle v^2\rangle$ are linear in T at high temperatures with corrections decreasing as $1/T^2$. $\langle x^2\rangle$ is weighted by ω^{-2} and thus the slope of $\ln f(T)$ depends on the vibrational density of states to leading order. $\langle v^2\rangle$ goes to the temperature-independent equipartition value. The zero temperature limits give the effects of zero point motion:

$$\langle x^2\rangle = \frac{\hbar}{2M}\widetilde{\omega^{-1}} \qquad \text{and} \qquad \langle v^2\rangle = \frac{\hbar}{2M}\widetilde{\omega^{1}}. \tag{A.6}$$

In the literature, the Debye expression for $g(\omega)$ is often used [45]. In this approximation, $g(\omega)$ is parabolic up to the maximum frequency and zero afterwards. This maximum frequency in temperature units is the Debye temperature Θ_{D}. The integrals in $\ln f(T)$ and $\delta_{\mathrm{SOD}}(T)$ can be performed to fit measured data to Θ_{D}. Well above Θ_{D}, $-\ln f = k^2\langle x^2\rangle$ is approximated by $6E_{\mathrm{R}}T/k_{\mathrm{B}}\Theta_{\mathrm{D}}^2$. E_{R} is the recoil energy ($E_{\mathrm{R}} = E_\gamma^2/2Mc^2$, where E_γ is the gamma ray energy). In the same limit, $\delta_{\mathrm{SOD}}(T)$ decreases linearly with temperature but with a universal slope equal to $-3k_{\mathrm{B}}T/2Mc$.

If a linear region in the resonant area $a(T)$ at elevated temperatures is found, it can be easily converted into the recoilless fraction $f(T)$. A simple shift of $\ln a(T)$ so that the extrapolated zero Kelvin intercept of the linear region is at zero suffices to convert $\ln a(T)$ to $\ln f(T)$.

References

[1] Shechtman D, Blech I, Gratias D and Cahn J W 1984 *Phys. Rev. Lett.* **53** 1951
[2] Kalugin P A, Kitaev A Yu and Levitov L S 1985 *J. Physique Lett.* **46** L601
[3] Bak P 1985 *Phys. Rev.* B **32** 5764–72
[4] Bak P 1985 *Phys. Rev. Lett.* **54** 1517–9
[5] Levine D, Lubensky T C, Ostlund S, Ramaswamy S, Steinhardt P J and Toner J 1985 *Phys. Rev. Lett.* **54** 1520–3
[6] Janssen T 1986 *Acta Crystallogr.* A **42** 261
[7] Janssen T and Radulescu O 2004 *Ferroelectrics* **305** 179–84
[8] Lifshitz R, Abraham S B and Shechtman D (ed) 2008 Quasicrystals: the silver jubilee *Philosophical Magazine* vol 88 (London: Taylor and Francis)
[9] Kalugin P A and Katz A 1993 *Europhys. Lett.* **21** 921
[10] Lubensky T C, Ramaswamy R and Toner J 1985 *Phys. Rev.* B **32** 7444–52
[11] Gähler F, Koschella U, Hocker S, Roth J and Trebin H-R 2003 *Quasicrystals* (New York: Wiley–VCH) chapter 4.2, pp 338–63
[12] Widom M 2008 *Philosophical Magazine* vol 88, ed R Lifshitz *et al* (London: Taylor and Francis) pp 2339–50
[13] Bancel P 1989 *Phys. Rev. Lett.* **63** 2741
[14] Bancel P 1989 *Phys. Rev. Lett.* **64** 496
[15] Francoual S, Livet F, Boissieu M De, Yakhou F, Bley F, Letoublon A, Caudron R and Gastaldi J 2003 *Phys. Rev. Lett.* **91** 225501
[16] Francoual S, Livet F, Boissieu M De, Yakhou F, Bley F, Letoublon A, Caudron R, Gastaldi J and Currat R 2006 *Phil. Mag.* **86** 35
[17] Feuerbacher M and Caillard D 2006 *Acta Mater.* **54** 3233–40
[18] de Boissieu M, Boudard M and Hennion B 1995 *Phys. Rev. Lett.* **75** 89
[19] Quivy A *et al* 1999 *Phys. Rev.* B **60** 6398
[20] Letoublon A *et al* 2001 *Phil. Mag. Lett.* **81** 273
[21] de Boissieu M 2006 *Phil. Mag.* **86** 1115
[22] Coddens G 2006 *Eur. Phys. J.* B **54** 37–65
[23] de Boissieu M *et al* 2008 *Philosophical Magazine* vol 88, ed R Lifshitz (London: Taylor and Francis) pp 2295–309
[24] Springer T 1972 *Quasielastic Neutron Scattering for the Investigation of Diffusive Motions in Solids and Liquids* (Berlin: Springer)
[25] Bée M 1988 *Quasielastic Neutron Scattering* (Bristol: Hilger)
[26] Hempelmann R 2000 *Quasielastic Neutron Scattering and Solid State Diffusion* (Oxford: Oxford Scientific)
[27] Vogl G, Mansel W and Dederichs P H 1976 *Phys. Rev. Lett.* **36** 1497–500
[28] Petry W and Vogl G 1982 *Z. Phys.* B **45** 207
[29] Vogl G 1990 *Hyperfine Interact.* **53** 197
[30] Coddens G, Soustelle C, Bellissent R and Calvayrac Y 1993 *Europhys. Lett.* **23** 33
[31] Lyonnard S, Coddens G, Calvayrac Y and Gratias D 1996 *Phys. Rev.* B **53** 3150
[32] Coddens G, Lyonnard S and Calvayrac Y 1997 *Phys. Rev. Lett.* **78** 4209
[33] Coddens G, Lyonnard S, Hennion B and Calvayrac Y 1999 *Phys. Rev. Lett.* **83** 3226–9
[34] Janot C, Magerl A, Frick B and de Boissieu M 1993 *Phys. Rev. Lett.* **71** 871
[35] de Araújo J H, Gomes A A and de Cunha J B M 1996 *Solid State Commun.* **97** 1025
[36] Coddens G, Lyonnard S, Sepiol B and Calvayrac Y 1995 *J. Physique* I **5** 771–6
[37] de Boissieu M, Francoual S, Kaneko Y and Ishimasa T 2005 *Phys. Rev. Lett.* **95** 105503
[38] Quiquandon M, Quivy A, Devaud J, Faudot F, Lefebvre S, Bessiere M and Calvayrac Y 1996 *J. Phys.: Condens. Matter* **8** 2487–512
[39] Quivy A, Quiquandon M, Calvayrac Y, Faudot F, Gratias D, Berger C, Brand R A, Simonet V and Hippert F 1996 *J. Phys.: Condens. Matter* **8** 4223
[40] Quiquandon M, Calvayrac Y, Quivy A, Faudot F and Gratias D 1999 *Mater. Res. Soc, Quasicrystals Symp.* p 95
[41] Brand R A, Coddens G, Chumakov A I and Calvayrac Y 1999 *Phys. Rev.* B **59** R14145–8
[42] Brand R A, Dianoux A-J and Calvayrac Y 2000 *Phys. Rev.* B **62** 8849–61
[43] Simonet V, Hippert F, Brand R A, Calvayrac Y, Rodriguez-Carvajal J and Sadoc A 2005 *Phys. Rev.* B **72** 024214
[44] Saadi N, Faudot F, Gratias D and Legendre B 1995 *Proc. 5th Int. Conf. on Quasicrystals (Avignon 1995)* (Singapore: World Scientific) p 656
[45] Gütlich P, Link R and Trautwein A 1978 *Mössbauer Spectroscopy and Transition Metal Chemistry* (Berlin: Springer)
[46] Frick B, Magerl A, Blanc Y and Rebesco R 1997 *Physica* B **234–236** 1177
[47] Hippert F, Brand R A, Pelloth J and Calvayrac Y 1994 *J. Phys.: Condens. Matter* **6** 11189–209

[48] Stadnik Z M, Takeuchi T, Tanaka N and Mizutani U 2003 *J. Phys.: Condens. Matter* **15** 6365–80
[49] Stadnik Z M and Wang P 2006 *J. Phys.: Condens. Matter* **18** 8383–94
[50] Brand R A, Pelloth J, Hippert F and Calvayrac Y 1999 *J. Phys.: Condens. Matter* **11** 7523–43
[51] Brand R A, Dianoux A-J, Calvayrac Y, Parshin P P and Zemlyanov M 2001 *The ILL Millennium Symposium and European User Meeting Proceedings* (Grenoble: ILL) p 132
[52] Parshin P P, Zemlyanov M G, Mashkov A V, Brand R A, Dianoux A-J and Calvayrac Y 2004 *Phys. Solid State* **46** 526
[53] Jena P 1976 *Phys. Rev. Lett.* **36** 418
[54] Christiansen J, Heubes P, Keitel R, Klinger W, Loeffler W, Sander W and Witthuhn W 1976 *Z. Phys.* B **24** 177
[55] Nishiyama K, Dimmling F, Kornrumpf Th and Riegel D 1976 *Phys. Rev. Lett.* **37** 357
[56] Sears V F 1986 *Methods of Experimental Physics: Neutron Scattering* vol 23A (Orlando, FL: Academic) p 521
[57] Edagawa K and Kajiyama K 2000 *Mater. Sci. Eng.* A **294–296** 646–9
[58] Edagawa K, Kajiyama K, Tamura R and Takeuchi S 2001 *Mater. Sci. Eng.* A **312** 293–8
[59] Shulyatev D A, Nigmatulin A S, Lobanova A V and Gasparyan T A 2008 *Phil. Mag.* **88** 2319–23
[60] Simonet V, Hippert F, Brand R A, Calvayrac Y, Rodriguez-Carvajal J and Sadoc A 2006 *Phil. Mag.* **86** 573
[61] Dahlborg U, Howells W S, Calvo dahlborg M and Dubois J M 2000 *Mater. Sci. Eng.* A **294–296** 670–4
[62] Coddens G 2001 *J. Phys.: Condens. Matter* **13** 8869
[63] Dahlborg U, Howells W S, Calvo dahlborg M, Dolinsek J and Dubois J M 2001 *J. Phys.: Condens. Matter* **13** 8873–4
[64] Sepiol B and Vogl G 1995 *Hyperfine Interact.* **59** 149
[65] Van Tendeloo G, Van Heurck C and Amelinckx S 1989 *Solid State Commun.* **71** 705–10
[66] Turchin V F 1963 *Soviet Progress in Neutron Physics* ed P A Krupchitskii (New York: Consultants Bureau) p 55
[67] Squires G L 1996 *Introduction to the Theory of Thermal Neutron Scattering* (New York: Dover)
[68] Charles P, Mitchell H, Parker S F and Ramirez-Cuesta A J 2005 *Vibrational Spectroscopy with Neutrons: with Applications in Chemistry, Biology, Materials Science and Catalysis* (Singapore: World Scientific)
[69] Vogl G and Sepiol B 1999 *Hyperfine Interact.* **123/124** 595
[70] Mehrer H 2007 *Diffusion in Solids: Fundamentals, Methods, Materials, Diffusion-Controlled Processes* (*Springer Series in Solid-State Sciences* vol 155) (Berlin: Springer)
[71] Maradudin A A and Flinn P A 1962 *Phys. Rev.* **126** 2059–71
[72] Schiffer J P, Parks P N and Heberle J 1964 *Phys. Rev.* **133** A1553–7
[73] Steyert W A and Taylor R D 1964 *Phys. Rev.* **134** A716–22
[74] Litterst F J, Gorobchenko V D and Kalvius G M 1983 *Hyperfine Interact.* **14** 21 (Contains several typographical errors)
[75] Litterst F J, Afanas'ev A M, Aleksandrov P A and Gorobchenko V D 1983 *Solid State Commun.* **45** 963
[76] Yoshida Y, Menningen M, Sielemann R, Vogl G, Weyer G and Schröder K 1988 *Phys. Rev. Lett.* **61** 195–8
[77] Torumba D, Parlinski K, Rots M and Cottenier S 2006 *Phys. Rev.* B **74** 144304
[78] Coddens G and Steurer W 1999 *Phys. Rev.* B **60** 270
[79] Edagawa K and Kajiyama K 2000 *Proc. 7th Int. Conf. on Quasicrystals (Stuttgart, 1999)* ed F Gähler, P Kramer, H-R Trebin, K Urban; *Sci. Eng.* A **294–296** 646
[80] Quiquandon M and Gratias D 2006 *Phys. Rev.* B **74** 214205
[81] Housley R M and Hess F 1966 *Phys. Rev.* **146** 517